

Article

Characterization and Assessment of Performance of Innovative Lime Mortars for Conservation of Building Heritage: Paimogo's Fort, a Case Study

Ana Rita Santos ¹, Maria do Rosário Veiga ^{1,*} and António Santos Silva ²

¹ Buildings Department, National Laboratory for Civil Engineering, 1700-066 Lisbon, Portugal; arsanos@lnec.pt

² Materials Department, National Laboratory for Civil Engineering, 1700-066 Lisbon, Portugal; ssilva@lnec.pt

* Correspondence: rveiga@lnec.pt

Abstract: Along the Portuguese coastline, several military fortifications were built with the intention to protect the territory from the constant military threat from the sea. These constructions have been subjected, during centuries, to a very aggressive environment; the renders, whose main function is the protection of walls, are particularly exposed to such actions. Nossa Senhora dos Anjos de Paimogo's Fort, better known as the Paimogo's Fort, is one of these fortifications, built in 1674 and classified of public interest since 1957. Within the scope of the "Coast Memory Fort" Project of EEA Grants Culture Programme 2014–2021, promoted by the Municipality of Lourinhã, repair mortars are being developed for the preservation of the Fort, considering the physical–mechanical and chemical characteristics of the pre-existing mortars and of the substrate, as well as the aggressive environmental conditions. In this work, several mortar compositions, compatible with the original mortars and designed to resist the aggressive environment, are briefly described and their main physical and mechanical characteristics are analysed and compared in successive ages. Different binder mixes were used, and a fine-tuning of the aggregate was carried out. Assessment of sequential wetting/drying cycles' effect on the mortar's behaviour is also presented. The laboratory results reveal that mortars with additions of 30% of quicklime present the best behaviour (with the lowest water absorption and highest strength). Moreover, the substitution of part of the siliceous sand by limestone aggregate, in general, increases the mortars' mechanical strength; however, the drying occurs slower, which could compromise the durability of these mortars if a good balance is not achieved.

Keywords: conservation; durability; innovative; lime; mortar; performance



Citation: Santos, A.R.; Veiga, M.d.R.; Santos Silva, A. Characterization and Assessment of Performance of Innovative Lime Mortars for Conservation of Building Heritage: Paimogo's Fort, a Case Study. *Appl. Sci.* **2023**, *13*, 4679. <https://doi.org/10.3390/app13084679>

Academic Editor: José Marcos Ortega

Received: 15 March 2023

Revised: 31 March 2023

Accepted: 1 April 2023

Published: 7 April 2023



Copyright: © 2023 by the authors. Licensee MDPI, Basel, Switzerland. This article is an open access article distributed under the terms and conditions of the Creative Commons Attribution (CC BY) license (<https://creativecommons.org/licenses/by/4.0/>).

1. Introduction

Located on the cliffs of Paimogo beach, in Lourinhã municipality, Portugal, Paimogo's Fort was classified as a Building of Public Interest since 1957. Designed to defend the north coastline of Lisbon from Cascais to Peniche, it was built in 1674, by decision of the 3rd Count of Cantanhede, and belongs to a large set of fortifications of the 2nd defensive line of Tagus River [1]. This historical construction, which was abandoned after the Liberal Wars (1832–1834), has been subjected to a very aggressive environment due to the proximity of the sea: salty water spray, high humidity, intense sun radiation, thermal shock, and strong winds. Mortar renders, whose main function is the protection of walls, are particularly exposed to such actions that make them especially susceptible to degradation over time (Figure 1).

Promoted by Lourinhã Municipality, the "Coast Memory Fort of Paimogo" European Economic Area (EEA) Grants project aims to safeguard and revitalize Paimogo's Fort. For this purpose, an analysis of the original mortars and an assessment of the conservation condition of the Fort was carried out. Similar to the other Portuguese coastal fortifications

from the 17th and 18th centuries [2–5], it is proven that this Fort is very well constructed, with well-selected materials and craftsmanship. Samples collected in situ clearly show that the original mortars used for masonry and renders were mechanically resistant and durable: they are based from calcitic air lime and mainly siliceous sand; shells were also found in their compositions, possibly from the local beach or fluvial sand deposits available near the fortification. Moreover, it was identified that the aggregate is free of clay. The binder/aggregate ratio varies depending on the type of mortar, ranging between 1:0.5:1 and 1:1:3 (lime:calcareous sand:siliceous sand, mass proportions). Considering the mortars performance, all compositions present high mechanical strengths (ranging between 2.5 and 5 MPa in compression) and moderate rate of water absorption (capillary water absorption coefficient between 0.4 and 1.7 kg/m²·min^{1/2}) [6,7].



Figure 1. Paimogo's Fort, in 2023.

However, in the intervention carried out in 2006, most of the original renders and plasters have been removed and replaced by new ones, which today present erosion and loss of cohesion. Thus, new repair mortars need to be formulated considering the physical–mechanical and chemical characteristics of the original mortars and of the masonry of the Fort, as well as the severe environmental conditions to which it is subjected; otherwise, there is a risk of accelerating degradation. For this reason, the formulation of replacement mortars is a complex process that must consider compatibility requirements, without neglecting the original appearance as well as adequate performance and durability.

In general, the repair mortars for this type of construction must have relatively high mechanical strength to resist erosion of the ocean wind and salt crystallization pressure, moderate elasticity modulus to accommodate deformations due to thermal variations, moderate capillary coefficient and high water vapour permeability to retard the entrance of water and allow a quick drying, as well as keeping compatibility characteristics. In addition, they should not have high contents of salts, to avoid the increase in salt contamination into the walls [8,9].

Several studies have pointed out the use of lime-based mortars as an appropriate and compatible solution for the rehabilitation of historical buildings [10–14]: lime-based formulations are chemically, physically, and mechanically compatible with the ancient mortars due to their similar composition, high porosity, and ability to accommodate movements from masonry structures. However, their development of mechanical strength is slower than for hydraulic mortars, since the hardening happens essentially by carbonation, which is a slow process and does not occur in saturated environments due to requiring diffusion of dissolved CO₂ through the mortar pore structure.

On the other hand, it is well known that cement mortars must be avoided whenever possible in rehabilitations works because they favour salt damage due to their content of alkali and sulphate ions, and they have excessive mechanical strength and elastic modulus that could transmit high stresses to a weaker substrate due to restrained shrinkage [15]

and the difficulty to follow the movements of the lime-based masonry. Moreover, cement mortars have lower water vapour permeability than lime-based materials, which limits the capacity to allow the evaporation of the capillary or adsorbed water in the wall [16], besides having a very distinct final appearance (in terms of colour and surface texture). However, in a similar case study, a lime-white cement mortar was applied in two thin coats of 1:1:6, as base coat, and 1:2:9, as the finishing coat (cement:lime:siliceous aggregate, by volume), with acceptable results for the last 30 years [17].

Other alternative innovative lime mortars solutions can be used for this case study, as suggested by Antoine-Joseph Lorient; in the 17th century, the author proposed the addition of quicklime to hydrated lime mix to increase its mechanical strength and provide volume stability of the lime mortars [18], since the excess water of the mix is then consumed by the quicklime instead of evaporated, avoiding macroporosity (typical of the lime mortars). However, a recent study by Magalhães et al. [19] showed cracking and degradation problems in mortars with this type of mix.

In the last decades, great attention was focused on enhancing the behaviour of lime mortars with the addition of nano products, such as nanosilica [20–27]. An important effect of the use of nanosilica in a lime mortar is the fast pozzolanic reaction, and consequently, the increase in its strengths [20–23]. Moreover, some studies report the positive impact of nanosilica on the mortars durability when subjected to laboratory weathering tests (temperature and relative humidity cycles, rain, UV light tests, and freezing resistance cycles) [24], as well as against sodium salts attack [25]. However, due to the very high specific surface of the nanosilica, it is expected to lead to high water/binder ratios, which will increase the coarse porosity and decrease the mortars' mechanical performance [25,26].

Other industrial pozzolanic additions, such as metakaolin, could be also an alternative solution for these repair mortars [28]; however, in some literature reviews, it was observed that lime-metakaolin may lose strength in the long term [29–31], which was demonstrated in the results of a similar case study in a fortification near Lisbon that present high levels of degradation after 20 years of its application [32].

Therefore, choosing durable and sustainable new renders for these constructions is a challenging situation. In this investigation, several lime-based mortars compositions are proposed and characterised with the aim of selecting a compatible and sustainable mortar that is durable to the aggressive environment for the restoration of Paimogo's Fort. Their main physical characteristics—capillary absorption and open porosity—and mechanical characteristics—flexural and compressive strength and dynamic elastic modulus—are analysed and compared at 28, 90, and 180 days. Moreover, to improve the mortar properties, a fine-tuning of the aggregate was carried out in two mortar compositions, which showed the best performance when compared to the other compositions.

2. Materials and Methods

2.1. Materials and Mortar Compositions

Several mortar formulations were studied in the process of selecting adequate repair mortars, in order to fulfil the requirements of compatibility with the ancient masonry and renders from the physical, mechanical, and chemical points of view [33,34] while ensuring adequate durability.

Since the original mortars were based from calcitic air lime with clay-free siliceous sand [6], the first mortar formulations were based from lime with natural siliceous sand (RT) from the Tagus River, supplied by Lena Agregados, SA.

Moreover, several lime lumps, measuring a few centimetres, were also found in the renders (Figure 2), suggesting that the lime was not well mixed during the mortar kneading or was prepared by a hot-mixing procedure [35]. Using a lower burning temperature could confer highly reactive lime with good plasticity and workability [36], as well as some physico-mechanical properties to the mixture, that favour the overall compatibility of the system [37].



Figure 2. Lime lumps found in the renders of Paimogo's Fort.

The properties of the raw materials are presented in Table 1.

Table 1. Identification and properties of the raw materials.

	Material Identification	Acronym	Bulk Density (kg/m ³)
Binder	Calcium hydrated lime (in powder form) CL90-S	A	359
	Calcium quicklime_CL90-Q (R5, P2)	Q	729
	Natural hydraulic lime_NHL 5	NHL	782
	White Portland-limestone cement_CEM II/B-L 32.5R	C	926
Sand	Natural siliceous sand from Tagus River 0/2 mm	RT	1448
	Calcareous sand 0/1 mm	C	1308
	Mix of 70% RT and 30% C sand	M ₁	1517
	Mix of 90% RT and 10% C sand	M ₂	1479
	Mix of 95% RT and 5% C sand	M ₃	1470
nano-SiO ₂	Aqueous colloidal dispersion of nano-sized silica 10/20 nm	NS	57

Therefore, to approach the original mortar compositions, lime-based mortars with slaked air lime (A) and slaked air lime + quicklime (A+Q) were formulated in this study, using a binder/aggregate ratio (in volume) of 1:2. Further, to give some hydraulicity and additional strength to the mortars to be applied in this severe marine environment, slaked air lime mortars with the addition of nanosilica (A+NS) were considered using approximately the same binder/aggregate ratio as the reference mortars. The proportions of quicklime and nanosilica were chosen according to previous research works [19,21,22] and also taking into account previous exploratory practical tests in laboratory, carried out with lime pastes, conducted to choose proportions of slaked lime-quicklime and lime-nanosilica that minimize shrinkage. Beyond that, moderately hydraulic mortars mixes as White Portland cement + slaked air lime (C:A) and natural hydraulic lime (NHL) mortars, with a binder/aggregate ratio (in volume) of 1:3:12 and 1:3, respectively, were also used [13].

Furthermore, as calcareous shells were detected in the original mortars [6], and in order to align more closely with the original formulation, as well as to improve the mortar's performance, a fine-tuning of the aggregates, substituting part of the siliceous sand by limestone aggregate in 30% (M₁), 10% (M₂) and 5% (M₃), by volume (Table 2 and Figure 3), was made into two mortars compositions, A+Q30% and C:A.

Table 2. Mortar compositions.

Mortar Identification	b/a Ratio (by Volume)	Composition	
slaked air lime	A	1:2	Slaked air lime:natural siliceous sand
slaked air lime + quicklime (%vol of lime)	A+Q10%	(1:0.1):2.2	Slaked air lime with 10% (by volume of lime) of quicklime:natural siliceous sand
	A+Q30%	(1:0.3):2.6	Slaked air lime with 30% (by volume of lime) of quicklime:natural siliceous sand
	A+Q30%:M ₁ (30%)	(1:0.3):(1.8:0.8)	Slaked air lime with 30% (by volume of lime) of quicklime:mix of 70% of natural siliceous sand plus 30% of calcareous sand
	A+Q30%:M ₂ (10%)	(1:0.3):(2.3:0.3)	Slaked air lime with 30% (by volume of lime) of quicklime:mix of 90% of natural siliceous sand plus 10% of calcareous sand
	A+Q30%:M ₃ (5%)	(1:0.3):(2.5:0.1)	Slaked air lime with 30% (by volume of lime) of quicklime:mix of 95% of natural siliceous sand plus 5% of calcareous sand
slaked air lime + nano-SiO ₂ (%wt of lime)	A+NS3%	(1:0.03):2	Slaked air lime with addition of 3% (by weight of lime) of nanosilica:natural siliceous sand
	A+NS5%	(1:0.05):2	Slaked air lime with addition of 5% (by weight of lime) of nanosilica:natural siliceous sand
slaked air lime + white cement	C:A	(1:3):12	White Portland-limestone cement:slaked air lime:natural siliceous sand
	C:A:M ₁ (30%)	(1:3):(8.4:3.6)	White Portland-limestone cement:slaked air lime:mix of 70% of natural siliceous sand plus 30% of calcareous sand
	C:A:M ₂ (10%)	(1:3):(10.8:1.2)	White Portland-limestone cement:slaked air lime:mix of 90% of natural siliceous sand plus 10% of calcareous sand
	C:A:M ₃ (5%)	(1:3):(11.4:0.6)	White Portland-limestone cement:slaked air lime:mix of 95% of natural siliceous sand plus 5% of calcareous sand
Natural hydraulic lime	NHL	1:3	Natural hydraulic lime:natural siliceous sand

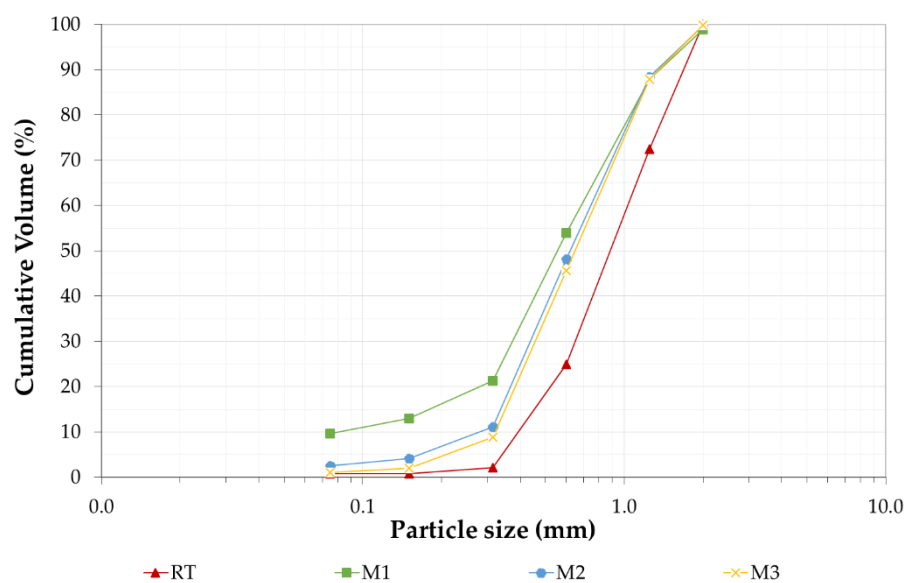


Figure 3. Grain size distributions of the used sands.

The mortar compositions are summarized in Table 2.

2.2. Preparation and Curing

The mortars were prepared in accordance with European standard EN 1015-2, using a mortar mixer Controls 65-L0005. However, with the use of the high percentage of quicklime in the formulation of the A+Q30% mortar, it was necessary to adapt the mixing process for these compositions, since it was not possible to apply the mortar after the mix using the standard method. In this case, the dry solid contents of the A+Q30% mortar (slaked air lime + quicklime:sand) were mixed before adding the predetermined amount of water to the dry solid mix into the mixer. The mix was prepared in three stages: at first, for a period of 5 min, with the mixer running at low speed; followed by a period of 10 min, where the mortar was left to rest; finally, the mixer was set to low speed for another 5-min period. Since the strong reaction of the quicklime happened a few minutes after the first mix, being—at this point—very difficult to apply the mortar, it was necessary to control the reaction of the quicklime by temperature measurements. It was found that after approximately 10 min of the first mix, the temperature in the interior of the mix decreases to 75 ± 5 °C, which at this point means it is again possible to mix the mortar to give it some plasticity.

For the preparation of the A+NS mortars, it was first necessary to homogenize the aqueous dispersion of nanosilica using a magnetic stirring for 5 min, followed by the continuous addition of the mixing water (quantity previously tested in laboratory) to the nanosilica, continuing magnetic stirring (500 rpm/minute) for 5 min more to obtain a homogeneous product. Once the gel was homogeneous with the water, it was added to the dry solid components and then mortars were prepared following the European standard [38].

All mortars were cast in normalized steel moulds ($40 \times 40 \times 160$ mm) and cured for 7 days in the moulds at 20 ± 2 °C and $65 \pm 5\%$ RH. In the first 3 days of curing, a sprinkling with water was performed on the mortar surface of each specimen every 24 h. After being removed from the moulds, the specimens were left to set and harden at the same hygrometric conditions until the test dates.

2.3. Characterization Methods

Several mortar properties in both fresh and hardened state were investigated and the test methods used are defined bellow. The results achieved for the hardened mortars were obtained at 28, 90, and 180 days.

Scanning electron microscopy (SEM) observations were also performed in some specimens using a TESCAN MIRA 3 field emission microscope, coupled with an energy dispersive spectrometer BRUKER XFlash 6-30 (EDS), on freshly fractured surfaces (using secondary electrons—SEI images).

2.3.1. Fresh Mortar Properties

The consistence of each mortar was optimised by experimental application on brick specimens with the criteria of using the minimum quantity of mixing water to allow good workability. After the determination of the optimum amount of water added, the consistency of the fresh mortars was measured by the flow table test, according to the EN 1015-3 [39]. The bulk density of the fresh mortars was also determined following the procedure used in the EN 1015-6 standard [40].

2.3.2. Physical Properties

The physical properties of the hardened mortars studied were the dry bulk density (ρ), following the European standard EN 1015-10 [41], and the open porosity by hydrostatic weighting (P_o), based on the EN 1936 [42] method but using a pressure of 40 kPa due to the low strength of lime mortars.

Three measurements were performed for each mortar type.

2.3.3. Mechanical Properties

The flexural (RT) and compressive (RC) strengths were determined according to the EN1015-11 standard [43] using an electromechanical testing device from PROET, model ETI-HM-S/CPC, with load cells of 2 kN for RT and 200 kN for RC.

The dynamic modulus of elasticity (E) of the mortars was also determined, by the fundamental resonance frequency method, based on EN 14146 [44], using the frequency of resonance ZRM ZEUS 2005 equipment.

The modulus of elasticity and the flexural strength were performed in three mortar prismatic specimens for each mortar type and the compressive strength tests were conducted on six half-prisms of each specimen resulting from the flexural test.

2.3.4. Hygric Properties

To study the water behaviour, capillary water absorption determination was carried out following the EN 15801 standard [45], where the prismatic specimens ($40 \times 40 \times 160$ mm) were placed in a container on non-absorbent small bars, with one of the $40 \text{ mm} \times 40 \text{ mm}$ faces in contact with tap water (approximately 10 mm deep). They were used without wrapping the lateral faces with paraffin. This methodology, which allowed to keep undamaged specimens for other tests at later ages, was considered acceptable as the results were comparable between all the mortars. The weight of absorbed water is measured until the difference between two successive weighing in 24 h is not greater than 1 wt.% of the mass of water absorbed by the specimen.

The water capillary absorption coefficient (CC), in $\text{kg}/\text{m}^2 \cdot \text{min}^{1/2}$, is calculated by the slope of the initial linear section of the capillary water absorption curve.

Immediately after the water absorption by the capillary test, the drying process of the specimens was conducted by measuring the weight loss over time, until the samples reached equilibrium with the environment conditions. From the drying curves, it was possible to determine the first (D_1 in $\text{kg}/\text{m}^2 \cdot \text{h}$) and the second (D_2 in $\text{kg}/\text{m}^2 \cdot \text{h}^{1/2}$) drying rates, based on EN 16322 [46], which characterize the transport of liquid water to the surface of the specimen (D_1), followed by a reduction in liquid water transport and progressive increase in the water vapour diffusion (D_2).

The first drying phase (D_1) is the negative slope of the initial linear part of the drying curve plotted against t (h) and was determined by linear regression, using at least three successive points. The second drying phase (D_2) is the negative slope of the linear section of the drying curve plotted against $t^{1/2}$ ($\text{h}^{1/2}$) and was determined also by linear regression, using at least three successive points.

Additionally, with the aim of investigating the effect of sequentially wetting/drying cycles in the mortars' compositions, three cycles of water absorption followed by drying were carried out in the same specimens, at 28, 90, and 180 days.

Three measurements were performed for each mortar type.

3. Results and Discussion

3.1. Fresh Mortars Properties

The water/binder (w/b) ratio used, and the obtained flow diameter and bulk density are presented in Table 3.

Table 3. Fresh mortars properties.

Mortar Identification		w/b Ratio (by Weight)	Flow Diameter (mm)	Bulk Density (kg/m ³)
slaked air lime	A	1.87	154 (2)	1933 (1)
slaked air lime + quicklime	A+Q10%	1.71	150 (3)	1945 (1)
	A+Q30%	1.71	145 * (4)	1916 (3)
	A+Q30%:M ₁ (30%)	1.55	151 * (2)	1979 (5)
	A+Q30%:M ₂ (10%)	1.81	149 * (3)	1906 (6)
	A+Q30%:M ₃ (5%)	1.81	149 * (2)	1901 (2)
slaked air lime + nano-SiO ₂	A+NS3%	1.81	142 (2)	1839 (2)
	A+NS5%	1.74	143 (2)	1815 (4)
slaked air lime + white cement	C:A	1.84	155 (3)	1971 (4)
	C:A:M ₁ (30%)	1.50	151 (1)	2052 (3)
	C:A:M ₂ (10%)	1.82	151 (2)	1970 (4)
	C:A:M ₃ (5%)	1.79	150 (2)	1959 (3)
natural hydraulic lime	NHL	1.10	153 (3)	1948 (3)

* Flow diameter after 10 min rest; (i) standard deviation reported in brackets.

According to the results in Table 3, the ideal water content for good workability was defined by ensuring that all lime-based mortars had a flow diameter of 150 ± 5 mm. The exception were the mortars with the addition of nanosilica (A+NS) that were considered as presenting good workability despite having smaller flow diameters. In fact, the application trials showed an adequate workability of lime-nanosilica mortars with a slightly lower water ratio than A mortar, even if the flow diameter was reduced from 154 mm to 142–143 mm. This could be due to their greater specific surface area (SSA) allowed by the nanosilica, thus requiring a higher water amount to wet all the surfaces. At the same time, the very small NS particles covering the coarser aggregates' surfaces decrease the friction among particles, providing a lubricant effect that enhances the plasticity and workability, even with low w/b ratios [47,48]. Thus, A+NS mortars did not evidence the need for a higher w/b ratio, despite their greater capacity to absorb water, resulting in their greater specific surface area (SSA).

Moreover, within the nanosilica mortars, increasing the wt% of nanosilica from 3 to 5% decreases the w/b ratio while keeping a similar flow diameter (142–143). The increase in NS particles may have contributed to fill the voids among coarser particles, thus reducing the water needs, which apparently contradicts some research [21,22].

Finally, substituting part of the siliceous sand by limestone aggregate, in general, leads to a reduction in mixing water (wt %), namely in mortar with 30% of sand substitution (M₁), without reducing the flow of the mortar. The reduction in the water content in air-lime mortars with calcareous sand, notwithstanding their higher SSA and rate of water absorption, is ascribed to a physical effect, where the raise of the smaller diameter particles of the limestone sand allows to fill the voids among the coarser particles of the siliceous aggregates, increasing the density, but also facilitating the movement of the coarse particles, as reported in previous studies regarding the addition of limestone filler in mortars [48,49]. In fact, very fine particles appear to have their own lubricating mechanism that requires less water than that needed by the larger particles to achieve similar flows [50].

3.2. Physical Properties

The determined physical properties of the mortars are listed in Table 4.

Table 4. Physical mortar properties.

Mortar Identification		Bulk Density (kg/m ³)			Open Porosity (%)		
		28d	90d	180d	28d	90d	180d
slaked air lime	A	1679 (3)	1704 (5)	1712 (2)	28 (0.1)	28 (0.2)	29 (0.1)
slaked air lime + quicklime	A+Q10%	1714 (4)	1736 (11)	1748 (5)	29 (0.5)	29 (0.2)	29 (0.2)
	A+Q30%	1715 (5)	1742 (5)	1760 (2)	27 (0.3)	27 (0.3)	27 (0.1)
	A+Q30%:M ₁ (30%)	1926 (27)	1826 (13)	1856 (10)	27 (0.2)	26 (0.2)	26 (0.2)
	A+Q30%:M ₂ (10%)	1696 (4)	1735 (3)	1739 (5)	28 (0.2)	27 (0.1)	28 (0.2)
	A+Q30%:M ₃ (5%)	1697 (2)	1739 (6)	1745 (9)	28 (0.2)	27 (0.2)	27 (0.1)
slaked air lime + nano-SiO ₂	A+NS3%	1623 (5)	1619 (2)	1635 (5)	34 (0.8)	35 (0.6)	35 (1.3)
	A+NS5%	1622 (5)	1564 (2)	1569 (2)	36 (0.1)	35 (1.0)	35 (0.3)
slaked air lime + white cement	C:A	1746 (7)	1766 (3)	1777 (5)	28 (0.2)	28 (0.1)	30 (0.5)
	C:A:M ₁ (30%)	1877 (7)	1893 (6)	1893 (7)	26 (1.2)	26 (0.1)	26 (0.2)
	C:A:M ₂ (10%)	1755 (9)	1773 (7)	1776 (9)	28 (0.2)	28 (0.3)	28 (0.3)
	C:A:M ₃ (5%)	1756 (5)	1774 (7)	1771 (14)	28 (0.6)	28 (0.2)	28 (0.2)
Natural hydraulic lime	NHL	1757 (2)	1767 (8)	1775 (7)	26 (0.1)	26 (0.2)	27 (0.2)

(i) standard deviation reported in brackets.

As expected, the density and the porosity of the mortars varies with their compositions (Figure 4): the mortars with the addition of NS (A+NS) showed the lowest values of density and the highest porosity, while the natural hydraulic lime (NHL) mortar showed the opposite behaviour. However, despite the lower value of open porosity, the NHL mortar is characterised by a regular microstructure with heterogeneous unconnected sub-rounded macropores (Figure 4d).

In general, in all mortar compositions, there was an increase in density with the curing age without significant changes in porosity, due to the carbonation reaction. However, in NS and A+Q30%:M₁ (30%) mortars, a small decrease was detected from 28 to 90 days, followed by an increase from 90 to 180 days.

Considering the use of different compositions, the addition of quicklime (A+Q30%) increases the bulk density (comparing with lower percentage), making the mortar more compact with low porosity (Figure 4b). In contrast, in the A+NS mortars, the density varies inversely with the concentration of the nanoparticles while the porosity, in general, presents similar values for both concentrations. This effect may be attributed to the introduction of air in the mix—due to the very small particles of nanosilica, as the closed big air bubbles do not contribute to open porosity—while reducing the density (Figure 4c).

The addition of white cement to the calcium lime mortar (C:A) leads to an increase in the dry bulk density without significant changes in the open porosity values between A and C:A mortars.

Considering the substitution of part of the siliceous sand by limestone aggregate, in general, the bulk density of C:A mortars increases and porosity decreases, namely in mortar with 30% of sand substitution (M₁), as expected, due to the packing of finer particles in the limestone aggregate. Similar to the C:A mortars, the open porosity is also reduced for the mortars with quicklime with 30% of sand substitution (M₁) (A+Q30%:M₁). However, in the lime mortar with quicklime with 10% and 5% of sand substitution (A+Q30%:M₂ and A+Q30%:M₃, respectively), there is a decrease in density and a slight increase in porosity; this behaviour could be ascribed to the different w/b ratio, which increases with these substitutions (Table 3) and consequently increases the porosity in the hardened state.

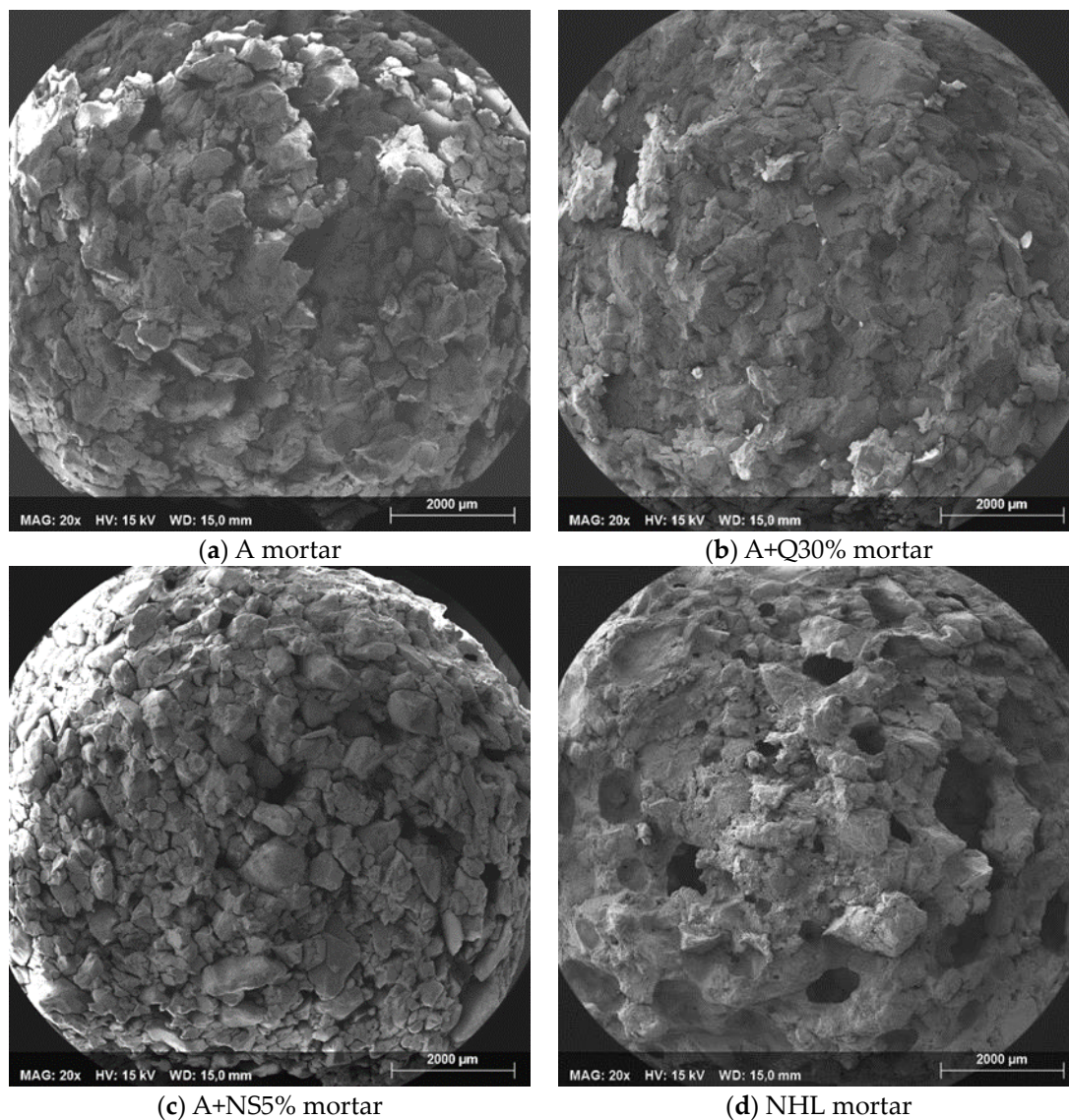


Figure 4. SEM images of the mortars' microstructure at low magnification, with a working distance (WD) of 15.0 mm. It is possible to observe the compact microstructure of the A (slaked air lime) mortar (a) and A+Q30% (slaked air lime with 30% of quicklime) mortar (b); the general microcracking on the A+NS5% (slaked air lime with addition of 5% of nanosilica) mortar is shown (c); as well as the heterogeneous microstructure of the NHL (natural hydraulic lime) mortar with few unconnected sub-rounded macropores (d).

3.3. Mechanical Behaviour

Figure 5 shows the mechanical properties values of the mortars, with different binders with siliceous sand, at 28, 90, and 180 days.

The results presented in Figure 5 indicate that all mortar compositions show relatively low mechanical strengths and moderate values of modulus of elasticity. Nevertheless, the strengths and the modulus of elasticity, in general, increase with the curing age, which is attributed to the progression of the carbonation reaction. However, in A+NS5% mortar, a noticeable increase in the compressive strength values could be observed at early curing times, and then a steep decrease was recorded at longer curing times.

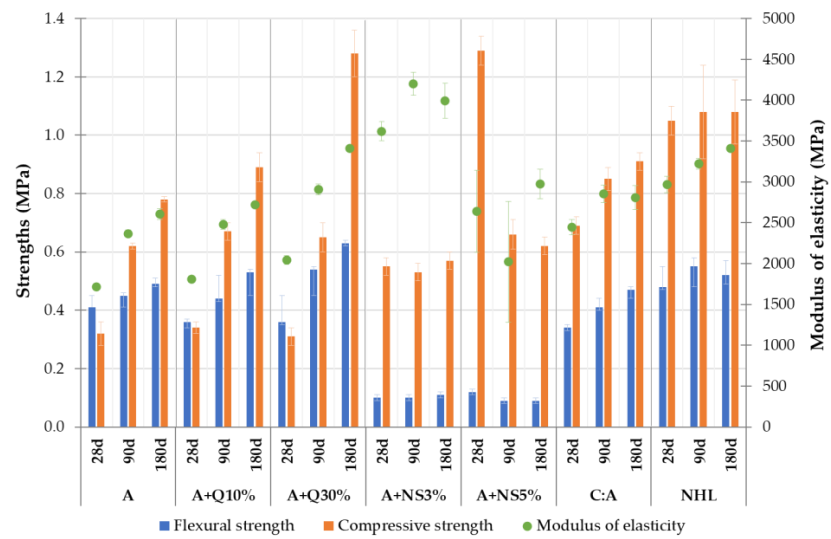


Figure 5. Mechanical properties of the mortars with siliceous sand.

Contrary to that observed in other studies with pozzolanic lime mortars [21,26], the additions of NS, namely with 5% wt, lead to a decrease in strength at latter ages as a result of drying shrinkage (Figure 6). This can be due to the pozzolanic reaction that absorbs a significant amount of water, associated with a dry curing, which negatively induces mortars microcracking, as shown in SEM images (Figure 7a), affecting its physical-mechanical properties [22,51].

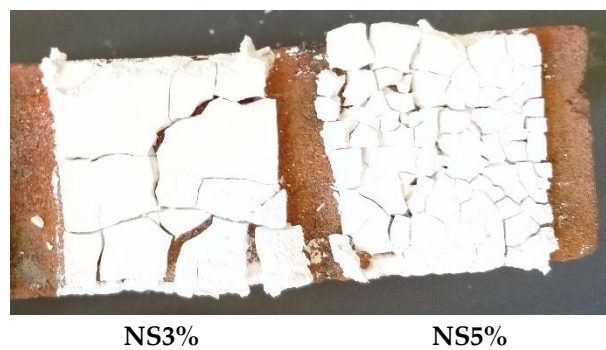


Figure 6. Cracking in lime paste applied on porous brick due to the effect of nanosilica.

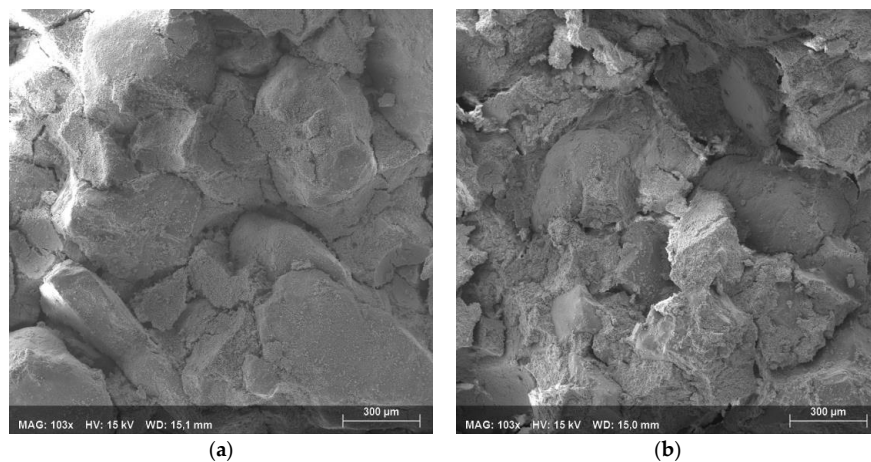


Figure 7. SEM images, at working distance (WD) of 15.0 mm, where it is possible to observe (a) the microcracking on the NS mortar; (b) compact microstructure of the A+Q30% mortar.

Mortar A is the most deformable; however, it has compressive strength values of the same order of magnitude as A+Q and A+NS mortars. Furthermore, if a small amount of cement is added (25%, in volume), the compressive strength of the mortars increases; however, the flexural strength is similar to that of lime mortar (A). The highest mechanical behaviour was obtained with the NHL mortar, and its strength is achieved at earlier ages compared to the air lime mortars. However, from 90 to 180 days, the A+Q30% mortar displays a significant evolution compared to other mortars compositions. This good behaviour of the A+Q30% mortar may confirm the literature argument [18] that quicklime absorbs the excess water from mixing in air lime mortars, thus reducing the drying shrinkage and consequently the microcracking during the drying process (Figure 7b), thus increasing the mechanical strength.

In what concerns the mechanical performances of the prismatic specimens with substitution of part of the siliceous sand by limestone aggregate (Figure 8), it is observed that the substitution is beneficial to the A+Q mortars; however, for the C:A mortar, the incremental improvement of the mechanical performance is only observed with 30% of sand substitution. As seen in previous studies [52,53], lime mortars prepared with limestone aggregate showed an increase in their mechanical strengths due to the crystallographic continuity between the limestone aggregate and the lime matrix [52].

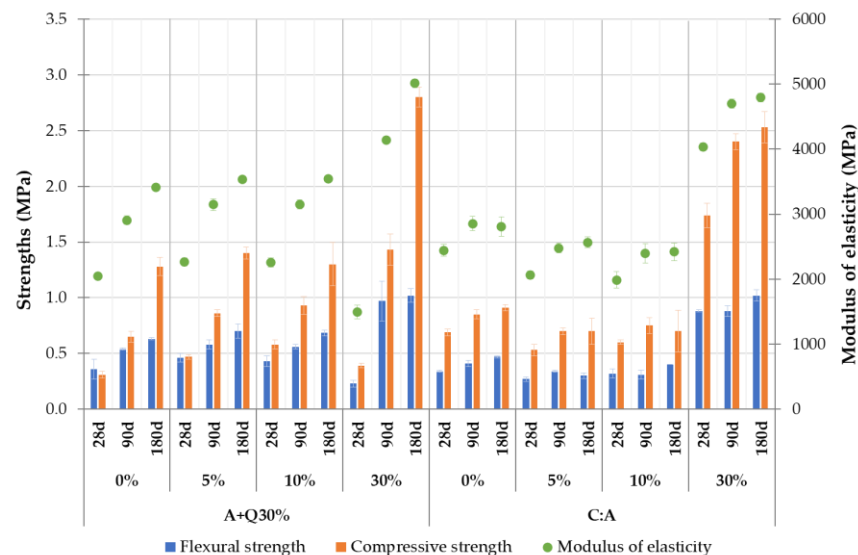


Figure 8. Mechanical properties of the A+Q30% and C:A mortars with substituting part of the siliceous sand by limestone aggregate.

3.4. Water Behaviour

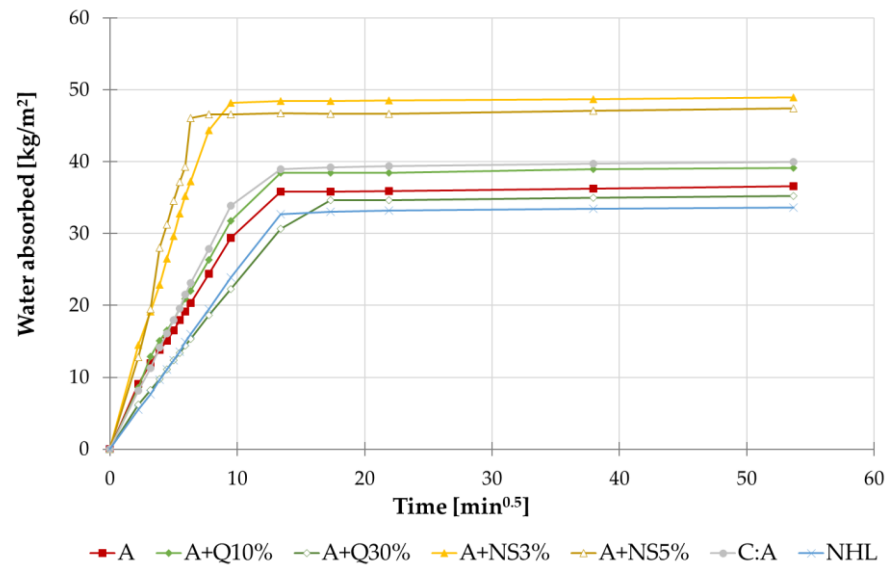
Table 5 reports the mean values of the capillary water absorption coefficient (CC), the asymptotic values (Abs.), and the drying rates (D_1 and D_2) for each mortar type at 28, 90, and 180 days. In Figures 9 and 10, the capillary water absorption and desorption curves of the mortars at 90 days are presented.

As shown in Table 5 and Figure 9, it is possible to observe that all mortar compositions have a high rate of water absorption in comparison with the results obtained in the original mortars of the Fort (capillary water absorption coefficient between 0.4 and 1.7 kg/m²·min^{1/2} [6]), which can make them more vulnerable to degradation. Nevertheless, in some mortar compositions, the capillary water absorption coefficient tends to decrease with the curing time due to the progression of carbonation.

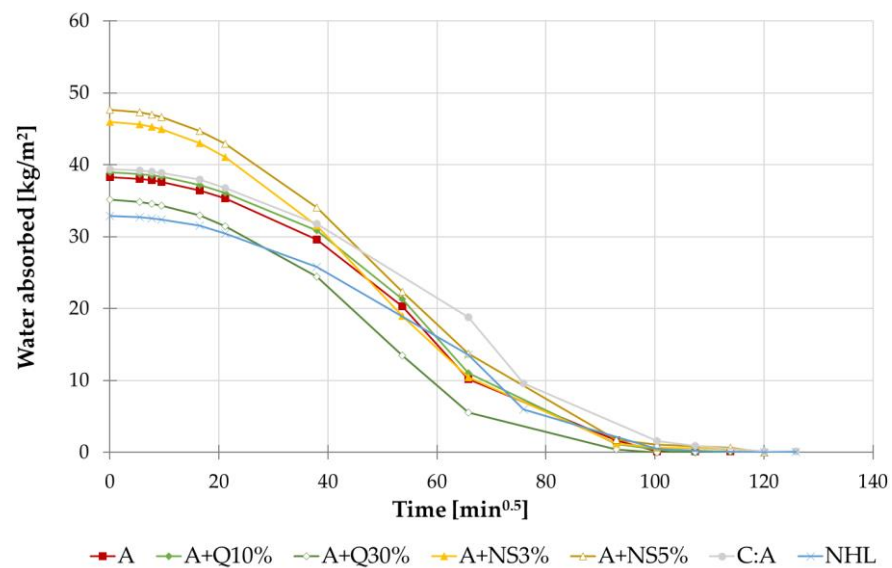
In general, the highest values of water absorption were observed in mortars with the addition of NS (A+NS), in agreement to the increase in the porosity (Table 4). However, the drying occurs faster than for the other mortars (high drying rates D_1 and D_2).

Contrarily, the lime mortar with quicklime (A+Q) and the natural hydraulic lime mortar (NHL) showed the lowest capillary water absorption coefficients and induced lower

values of water absorption, attributed to the slight decrease in porosity and probably due to the main volume of pores being slightly shifted towards smaller diameters in the capillary range, in comparison with the other mortars, which have a significant influence on the transport processes of water [54].



(a)



(b)

Figure 9. Capillary water absorption curves of the mortars with siliceous sand at 90 days: (a) water absorption; (b) water desorption.

Table 5. Results of capillary water absorption and drying rates of the mortars.

Mortar Identification	Capillarity Coefficient			Water Absorbed			Drying Rates					
	CC (kg/m ² ·min ^{1/2})			Abs (kg/m ²)			D ₁ (kg/m ² ·h)			D ₂ (kg/m ² ·h ^{1/2})		
	28d	90d	180d	28d	90d	180d	28d	90d	180d	28d	90d	180d
A	3.3	3.0	3.1	39.2	37.2	38.5	0.54	0.38	0.31	3.73	3.96	2.68
A+Q10%	3.3	3.3	2.9	37.7	39.9	39.3	0.49	0.38	0.25	6.08	5.14	4.74
A+Q30%	2.5	2.3	2.3	36.9	35.5	36.2	0.44	0.42	0.31	5.90	5.27	4.69
A+Q30%:M ₁ (30%)	1.1	1.7	1.9	27.7	36.2	36.0	0.20	0.18	0.28	4.05	3.57	3.25
A+Q30%:M ₂ (10%)	2.0	1.9	1.9	37.8	35.3	36.4	0.24	0.21	0.22	4.04	4.28	5.82
A+Q30%:M ₃ (5%)	1.9	2.0	1.9	37.8	37.0	36.3	0.20	0.20	0.21	4.36	4.62	5.94
A+NS3%	4.2	5.7	5.3	41.5	49.4	45.9	0.50	0.56	0.45	5.16	5.41	4.69
A+NS5%	2.6	7.2	5.8	37.0	48.1	48.0	0.51	0.53	0.38	4.87	5.13	4.97
C:A	3.7	3.6	3.6	42.2	40.6	40.9	0.50	0.29	0.36	4.60	4.35	3.12
C:A:M ₁ (30%)	2.0	2.4	2.6	36.1	36.0	36.7	0.25	0.37	0.24	4.09	5.19	2.35
C:A:M ₂ (10%)	2.9	3.0	3.0	40.5	39.9	40.5	0.32	0.21	0.53	4.37	4.77	4.89
C:A:M ₃ (5%)	2.9	2.8	2.8	40.2	37.6	38.8	0.37	0.21	0.55	3.61	3.97	4.99
NHL	2.2	2.5	2.5	33.4	34.1	34.9	0.48	0.28	0.36	4.46	3.91	2.75

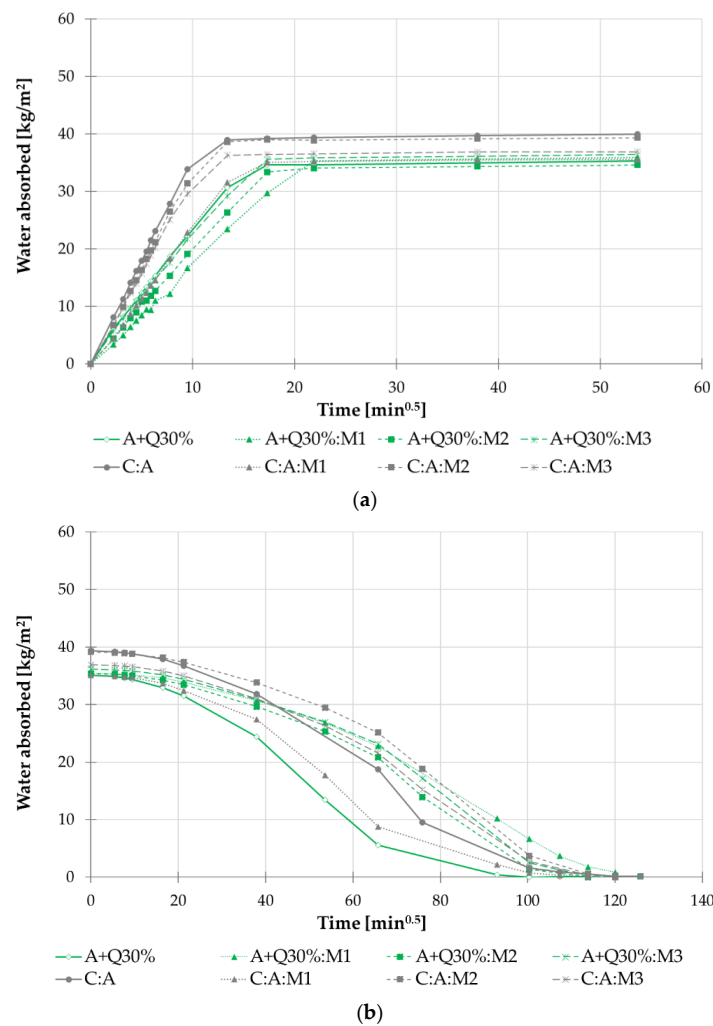


Figure 10. Capillary water absorption curves of the mortars with fine-tuning of the aggregate, at 90 days: (a) water absorption; (b) water desorption.

Despite the results of the drying rates being very heterogeneous, in general, the NHL mortar also shows the lowest drying rates, which means that the drying also occurs slower. On the other hand, regarding the mortars with quicklime (A+Q), the results generally show that the first drying phase (D_1) occurs slower and the relative high values of the second drying rate (D_2) indicates higher water vapour diffusion. The low D_1 and high D_2 may indicate a predominance of small capillary pores that slow down the first phase of desabsorption and thus increases the mechanical strengths (Figure 4b).

The fine-tuning of the aggregate substituting part of the siliceous sand by limestone aggregate (Table 5 and Figure 10) decreases in general, as expected, the rate of water absorption of the two mortars and the drying also occurs slower, related to the filler effect, where the voids in the siliceous sand are filled by the calcareous sand. This effect could increase the volume of capillary porosity and lead to a reduction in the main pore diameter. Nonetheless, even though the porosity variations were relatively low, namely with M_2 and M_3 substitutions in A+Q mortars, a slight increase in the total water absorption was observed, namely at early ages. In all the C:A mortars with sand substitution, a decrease in the total water absorption was revealed, attributed to the presence of hydraulic compounds that could reduce, even more, the volume and the diameter of capillary pores.

3.5. Assessment of the Sequential Wetting/Drying Cycles

To assess the mortars' performance subjected to cycles of water absorption/desabsorption, as they will be subjected in real environment conditions, test specimens were submitted, in laboratory conditions (20 ± 2 °C and $65 \pm 5\%$ RH), to cycles of capillary water absorption followed by drying at different curing ages: 28 (1st cycle), 90 (2nd cycle), and 180 (3rd cycle) days.

In the analysis, the following aspects were considered:

- (i) Determination of the parameters of water absorption coefficient (CC), asymptotic values (Abs.), and drying rates (D_1 and D_2), and compared with specimens that were not subjected to the cycles.
- (ii) Qualitative evaluation, based on visual appearance, during the capillary water absorption/desabsorption test.

Regarding the results shown in Figure 11, which shows the capillary water absorption (Figure 11a) and desorption (Figure 11b) values of the mortars after the cycles, with the exception of the mortars with NS, in general, the capillary water absorption coefficient (CC) slightly decreases with the cycles of absorption. This behaviour can be related not only to the progression of carbonation, but also to the reactions of dissolution and reprecipitation of the carbonated binder [5] (Figure 12).

For the drying cycles, this trend is not so clear; however, except for the A+Q30% and A+NS mortars, after the 2nd cycle, all mortars tend to have an increase in their first drying rate (D_1). This behaviour could be ascribed to the transformation of portlandite into calcium carbonate fulfilling the largest pores which, in general, increase the volume in the capillary porosity range, with a reduction in the main pore diameters [53].

The different behaviour of the mortars with NS is consistent with the previous mechanical and physical results. In fact, this performance can be attributed to the microcracking on the aggregate/binder interface, associated to shrinkage strains (Figure 7a), which leads to a coarsening of pore diameters [55,56]. Moreover, in the presence of water, the specimens with nanosilica became so fragile that they were broken during the measurements.

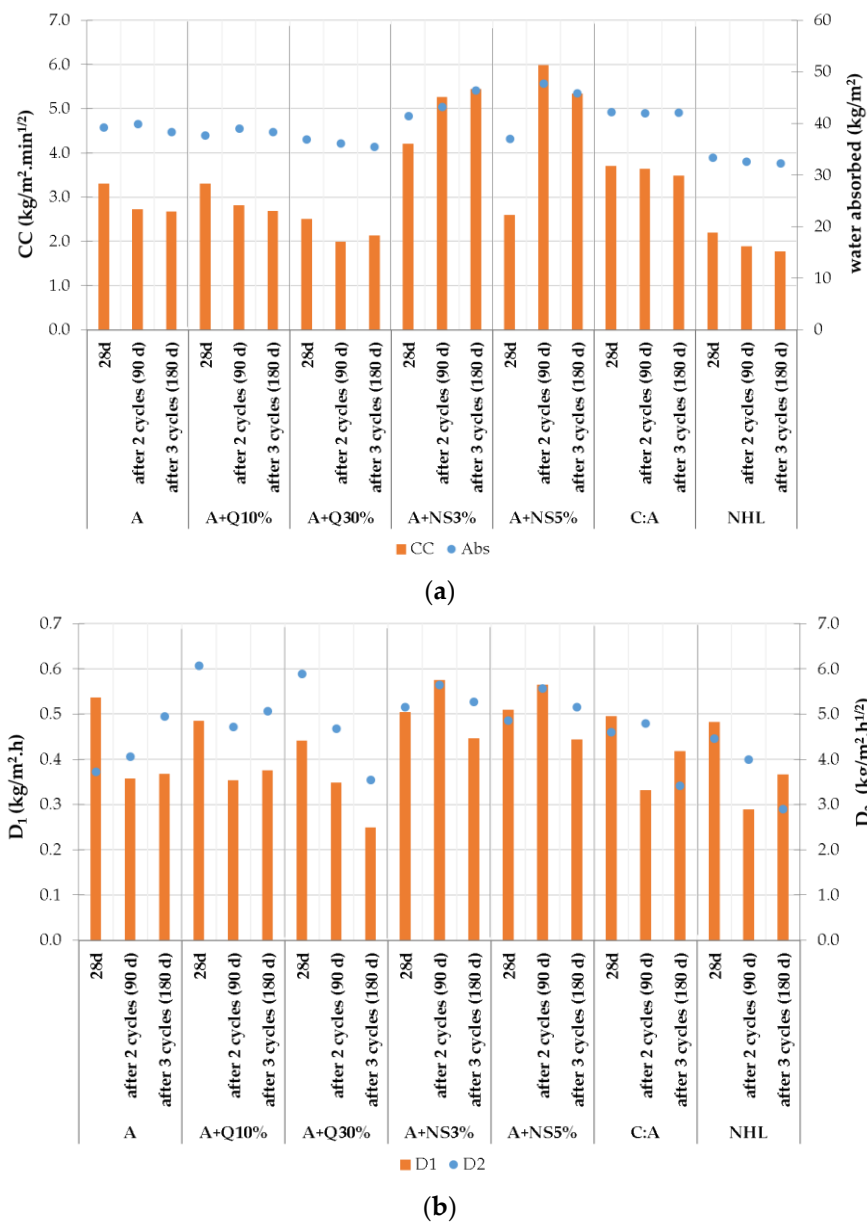


Figure 11. Hydric properties of the mortars with siliceous sand, after cycles of the water absorption: (a) water absorption; (b) water desorption.

Considering the use of limestone aggregate (Figure 13), as reported before, in general, the rate of water absorption of the two types of mortar decreases and the drying occurs slower. Furthermore, except for the sand substitution of 30% (M_1), the number of cycles improves the mortar performances with a reduction in the rate of absorption and of the total water absorption. However, there is a decrease in the water flow, and consequently a decrease in D_1 , and thus the values of D_2 increase from the first to the second cycle, which represents the reduction in liquid water transport and progressive increase in water vapour diffusion, probably due to the volume decrease in large capillary pores owing to the carbonation process (Figure 14).

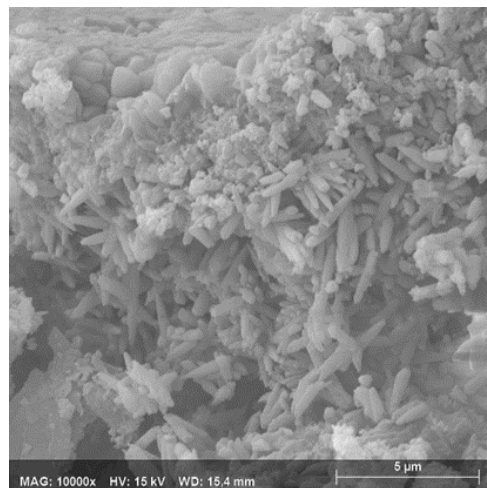


Figure 12. SEM image at high magnification (MAG: 10,000x), with a working distance (WD) of 15.4 mm, at A mortar surface where it is possible to observe the presence of different calcium carbonate crystals, some with an acicular shape attributed to phenomena of dissolution and reprecipitation of the carbonated binder.

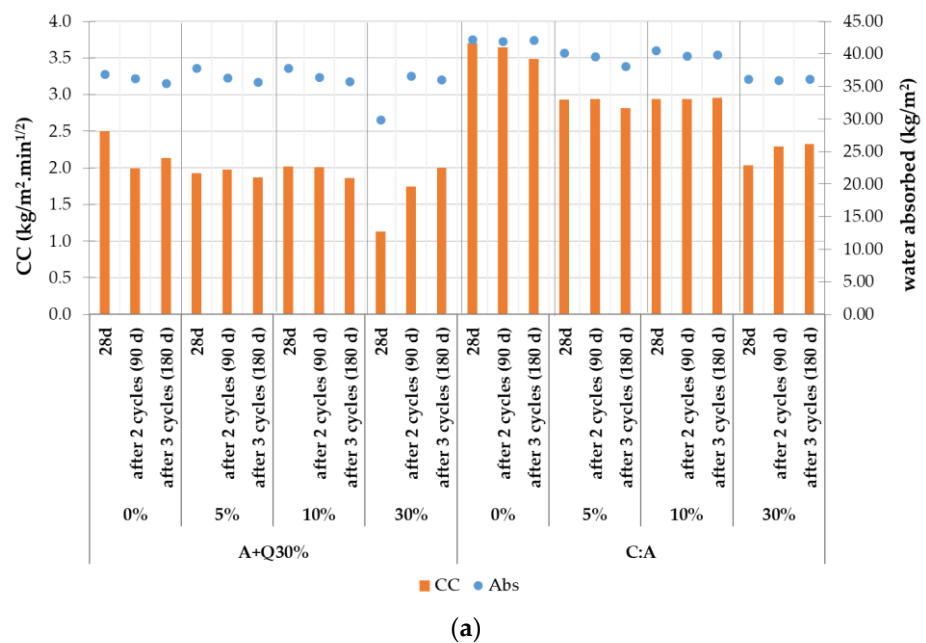


Figure 13. Cont.

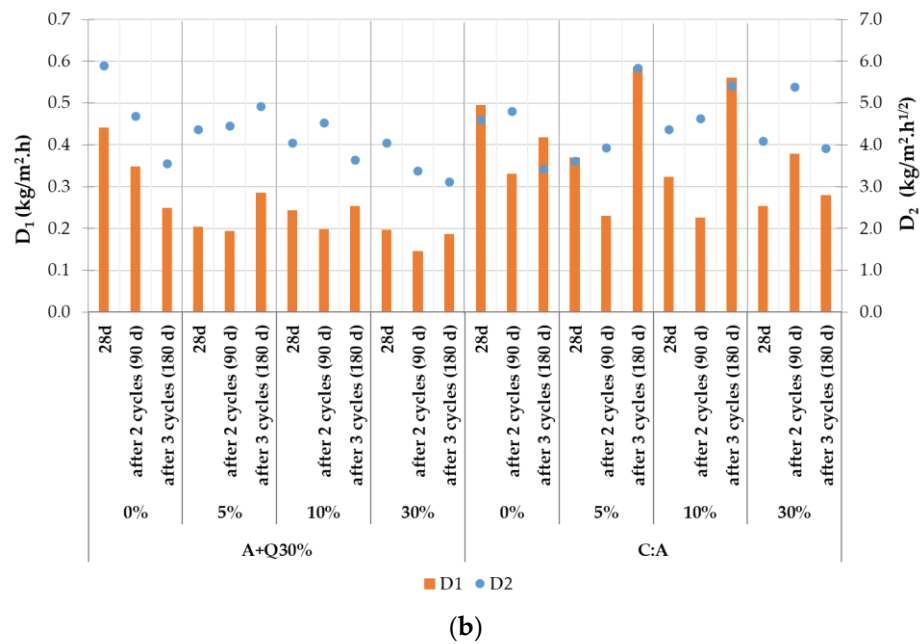


Figure 13. Hydric properties of the mortars with fine-tuning of the aggregate, after cycles of the water absorption: (a) water absorption; (b) water desorption.



Figure 14. SEM image with a magnification of the 3500x and a working distance (WD) of 14.9 mm at A+Q30%:M₂ mortar where it is possible to observe the large capillary pores filled by carbonate crystals after cycles.

The visual assessment of mortars reveals that during the second cycle of water absorption, a pink colouration appears on the C:A:M₂ and C:A:M₃ mortar specimens (Figure 15a), probably due to the presence of microbiological contamination, able to produce coloured compounds such as *Rhodotorula S.P.* or those closely related, which could lead to a biodeterioration of the mortars [57,58].

Furthermore, after the 3rd cycle, during the drying stage, mortars with quicklime (A+Q10% and A+Q30%) present black mould growth on the top of specimens (Figure 15b), while on the hydraulic mortars (C:A, C:A:Mi, and NHL), salt efflorescence occurs (sulphate and chloride) on the drying surface of the specimens (Figure 15c).

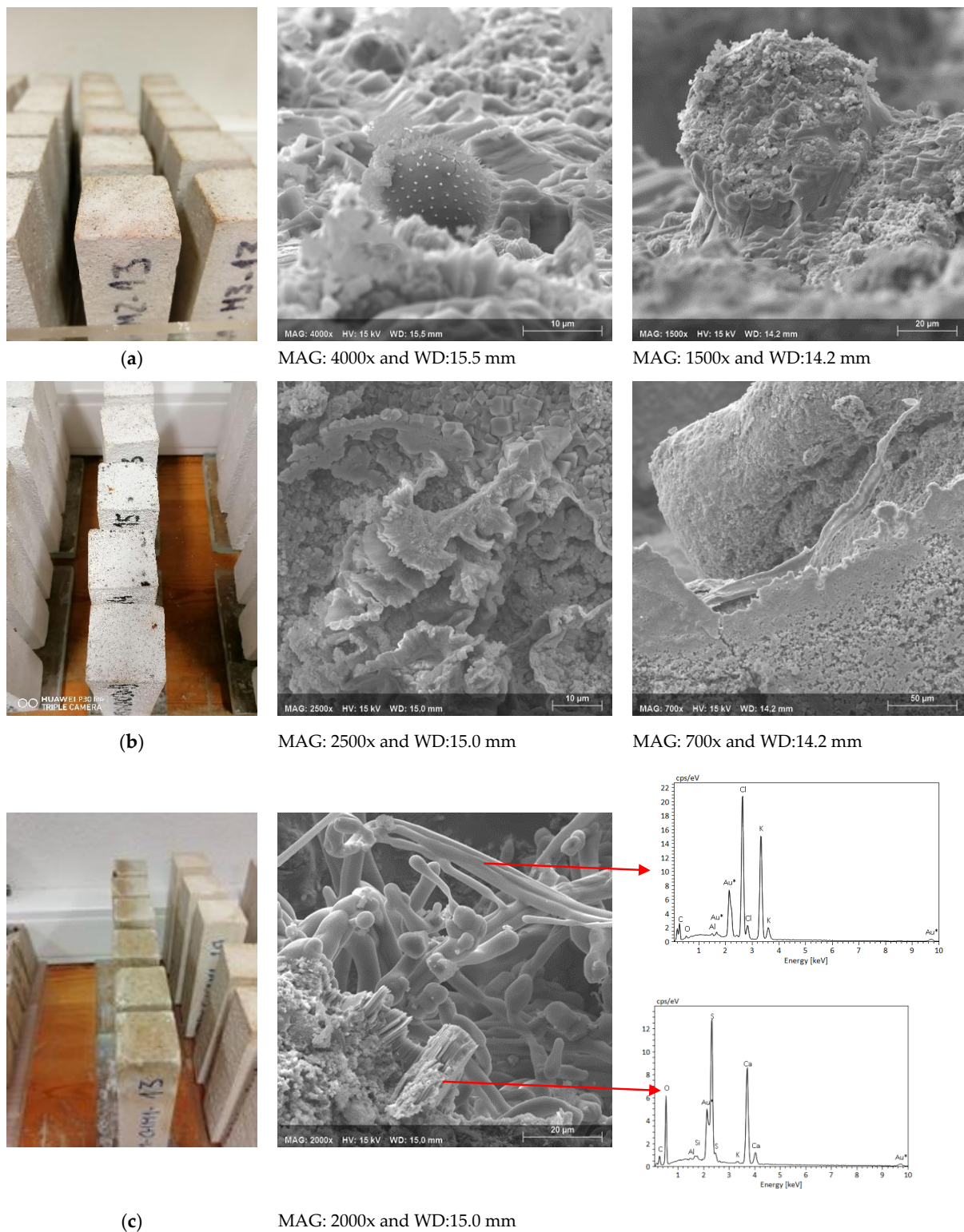


Figure 15. Damaging effect of the samples after the cycles: (a) rosy discolouration on the top of the C:A:M₂ and C:A:M₃ specimens and organic elements found at mortar surfaces in SEM observation; (b) black mould growth on the top of the A+Q10% and A+Q30% specimens and organic compounds found at mortar surfaces in SEM observation; (c) presence of salt efflorescences in the NHL specimens at SEM observation and EDS spectra, where the chemical element gold (Au*) is detected due to necessary recovering of the samples for the SEM analysis.

4. Global Discussion

According to these findings, considering the physical and mechanical results, it can be observed that the mortar with slaked air lime (A), despite its chemical and physical compatibility with the ancient renders, presents relatively low strengths and a high rate of water absorption, which could be a drawback in the environmental conditions of the Fort. However, these characteristics improve with the curing age.

Adding quicklime to the slaked air lime mortars (A+Q10% and A+Q30%), an increase in the mechanical strengths is observed, especially after 180 days. Furthermore, the additions of 30% of quicklime seems to have the most positive influence on the mortar performance, since there is a reduction in the capillary water absorption and the drying occurs relatively faster. Moreover, this composition presents a reduced w/b ratio that, consequently, reduces the porosity and improves the mechanical strengths in the hardened state, which are very important characteristics for the replacement mortar to be successful in this severe environment. However, after few cycles of capillary absorption/drying, black mould arises on the top of the A+Q specimens; therefore, the use of this composition in local areas with high levels of humidity should be analysed in detail in further studies.

Likewise, the additions of white cement to the slaked air lime mortars (C:A) also increases the mechanical strengths, namely at early ages, even with similar open porosity values as the A mortar. However, probably due to its large volume of capillary porosity, these compositions present higher values of water absorption and the drying also occurs slower than for the lime-based mortars.

In addition, the natural hydraulic lime mortar (NHL) shows greater mechanical strengths, even at early ages. However, despite the moderate values of water absorption, this composition shows a slower drying process. Additionally, the presence of soluble salts on the surface of the specimens after the capillary water absorption cycles could have mechanical repercussions and cause decay of the renders, as well as of the substrate.

A decrease in mortar performance is observed with the addition of nanosilica (A+NS3% and A+NS5%). In general, with early curing times, a noticeable increase in the compressive strength values could be observed, even with a very high percentage of porosity. However, at longer curing ages, a steep decrease was recorded, namely in the mortar with 5% of nanosilica (A+NS5%), which was related to the microcracking of the matrix associated to shrinkage strains, which could interfere in strength development in the long term, which can thus limit the use of NS in lime mortars for conservation purposes. This problem could probably be controlled with a humid long curing, but such conditions are very difficult to guarantee in real works. Moreover, mortars with the addition of NS present the highest values of water absorption, and their drying occurs faster than for the other mortars due to their high pore connectivity. Furthermore, when subjected to a few water absorption/desorption cycles, the specimens evidence high fragility.

Regarding the global results of the samples, the use of A+Q30% and C:A mortars seem to present the best global performance. Thus, in order to approach the original formulation with regard to its composition and grain size distribution, as well as improve the mortar performance, a fine-tuning of the aggregate, substituting part of the siliceous sand by limestone aggregate in 30% (M₁), 10% (M₂), and 5% (M₃) by volume was made. The laboratory results showed that the substitution, in general, decreases the porosity and increases the mechanical performance, as well as decreases the rate of water absorption of the two types of mortars, namely on mortar with 30% of sand substitution (M₁). However, with this sand substitution of 30% (M₁), the mortars suffer high shrinkage, which could lead to microcracking of the matrix, and consequently reduce its performance with the curing time. After some cycles of water absorption/drying, except for the sand substitution of 30% (M₁), the number of cycles improves the mortar performances (reduce the rate of absorption and the total water absorbed). However, there is a decrease in the water flow for all mortars, which may be responsible for the presence of microorganisms, detected namely in the C:A mortar surface with 10% and 5% of aggregate substitution.

5. Conclusions

Several mortar compositions, compatible with the original mortars and designed to be sustainable and resist the severe marine environment, were selected, using different binder mixes and aggregates, and their main physical and mechanical characteristics were analysed in laboratory conditions and compared at 28, 90, and 180 days.

This work showed that all specimens have, in general, good appearance, without cracking in laboratory conditions during the curing age. The exception are the lime mortars with nanosilica (A+NS), that evidenced significant cracking. In general, all the mortars present relatively low mechanical strengths, moderate values of modulus of elasticity, and high rates of water absorption at 28 days, but they also showed improved behaviour with increasing curing age.

In general, the slaked air lime mortar (A) shows some potential of improvement in the real environmental conditions of the Fort with salty water spray and thermal variation, due to its pore network with large pores and high connectivity, which allows fast drying and good performance to salt attack. However, its low mechanical characteristics and high rate of water absorption can compromise its durability due to the severe real environmental conditions, with strong winds that could cause erosion on the mortar surface.

With the aim to approach the original formulation and increase the mechanical strengths of the lime mortar (A), quicklime with 10% and 30% by volume of lime was added (A+Q10% and A+Q30%). The obtained results showed an improvement of the behaviour with moderate but higher strengths at later ages and lower water absorption rates, ascribed to a reduction in the volume and diameter of large capillary pores, namely with an addition of 30%.

A general detrimental strength development was detected in lime mortars with nanosilica (A+NS), namely with the addition of large amounts of NS (5% wt) in the lime mortar. Moreover, the addition of NS leads to an increase in porosity and high rates of water absorption. This behaviour was ascribed to the microcracking occurrence in these mortars and/or to the poor stability of the hydrated phases generated, which eventually impaired the strengths at latter ages. These results advise against its use for cultural heritage sites since they are more vulnerable to degradation and their behaviour is less stable.

The slaked air lime with white cement mortar (C:A) also shows mechanical strength improvements, namely at early ages, ascribed to the presence of hydrated compounds. However, probably due to its large volume of capillary porosity, this composition presents higher values of water absorption, as well as its drying occurring slower than that of lime mortars.

Therefore, the compositions A+Q30% and C:A seem to generally improve the mortar behaviour in comparison to the A mortar, increasing the mechanical strengths and, in some cases, reducing the water absorption. Hence, a fine-tuning of these compositions by substitution of part of the siliceous sand by different percentages of limestone aggregate were made. The results show increases in the mortars' mechanical strength and reductions in the rate of water absorption by capillarity, namely with 30% of substitution, due to their well-packed system. However, for all compositions, the drying occurs slower, which could compromise the durability of these mortars, such as the appearance of microorganisms in a very humid environment, if a good balance is not achieved.

The NHL mortars had a lower w/b ratio and consequently lower porosity than the air lime-based mortars. Therefore, besides the highest mechanical strengths and lowest capillary water absorption, they present a slower drying process and a possible trend to early degradation due to the salt crystallization.

Finally, the results of this study point to the potential adequacy of the mortars based on slaked air lime with the addition of quicklime or low percentages of white cement, and with partial substitution of siliceous aggregate by limestone aggregate, to be used in the restoration of the Paimogo Fort. Considering a more favorable drying behaviour, the A+Q30% presents the most adequate behaviour, as a whole.

However, further studies for the assessment of the mortar performances applied on porous substrates and in the real marine environment would be useful to fully support this last conclusion. To evaluate their behaviour and durability in real conditions, all mortar compositions will be applied on porous substrates, and their physical–mechanical behaviour will be assessed to select the most suitable rehabilitation mortar. Moreover, a new phase of tests is underway to assess the performance and durability of selected lime-based mortar formulations in the real environmental conditions of the Fort.

Author Contributions: A.R.S. performed the experiments in the laboratories of Portuguese National Laboratory for Civil Engineering; A.R.S. and M.d.R.V. analysed and discussed the fresh and hardened tests results; A.R.S. and A.S.S. analysed and discussed the SEM observations; M.d.R.V. and A.S.S. were responsible for the supervision of the research; Writing: original draft preparation was performed by A.R.S. and the review and editing was performed by M.d.R.V., A.S.S. and A.R.S.; M.d.R.V. was responsible for the funding acquisition. All authors have read and agreed to the published version of the manuscript.

Funding: Programme Cultural Entrepreneurship, Cultural Heritage and Cultural Cooperation of European Economic Area (EEA) grants, Culture Programme 2014–2021, within the scope of the “Coastal Memory Fort” project.

Institutional Review Board Statement: Not applicable.

Informed Consent Statement: Not applicable.

Data Availability Statement: Not applicable.

Acknowledgments: The authors wish to thank LNEC technicians for their collaboration in carrying out the tests, the collaboration of Lhoist Portugal and Secil Argamassas in supplying the testing materials, as well as the support and collaboration of Lourinhã Municipality. This work is a contribution to the EEA Grants Culture Programme 2014–2021 “Coastal Memory Fort—Paimogo Fort”.

Conflicts of Interest: The authors declare no conflict of interest.

References

1. Nossa Senhora dos Anjos de Paimogo’s Fort (Forte no Lugar de Paimogo/Forte de Nossa Senhora dos Anjos de Paimogo). (In Portuguese). Available online: http://www.monumentos.gov.pt/Site/APP_PagesUser/SIPA.aspx?id=6327 (accessed on 4 January 2023).
2. Santos Silva, A.; Veiga, M.R. Degradation and repair of renders in ancient fortresses close to sea. In Proceedings of the MEDACHS’ 08–1st International Conference on Construction Heritage in Coastal and Marine Environments: Damage, Diagnostics, Maintenance and Rehabilitation, Lisboa, Portugal, 28–30 January 2008; LNEC: Lisboa, Portugal, 2008.
3. Tavares, M.; Magalhães, A.C.; Veiga, M.R.; Velosa, A.; Aguiar, J. Repair mortars for a maritime fortress of the XVII th century. In Proceedings of the MEDACHS’ 08–1st International Conference on Construction Heritage in Coastal and Marine Environments: Damage, Diagnostics, Maintenance and Rehabilitation, Lisboa, Portugal, 28–30 January 2008; LNEC: Lisboa, Portugal, 2008.
4. Veiga, M.R.; Santos Silva, A.; Tavares, M.; Santos, A.R.; Lampreia, N. Characterization of Renders and Plasters from a 16th Century Portuguese Military Structure. *Restor. Build. Monum.* **2013**, *19*, 223–237. [CrossRef]
5. Borges, C.; Santos Silva, A.; Veiga, M.R. Durability of ancient lime mortars in humid environment. *Constr. Build. Mater.* **2014**, *66*, 606–620. [CrossRef]
6. Veiga, M.R.; Santos Silva, A.; Marques, A.I.; Sabala, B. *Characterization of Existing Mortars of the Fort of Nossa Senhora dos Anjos do Paimogo (Caracterização das Argamassas Existentes no Forte de Nossa Senhora dos Anjos do Paimogo)*; Report LNEC 67/2022—DED/NRI, Lisboa, Portugal, 2022; LNEC: Lisboa, Portugal, 2022; 114p. (In Portuguese)
7. Traditional Mortars of the Fort of Paimogo: Composition, Performance, Replication. Available online: <https://www.eeagrants.gov.pt/en/programmes/culture/news/traditional-mortars-of-the-fort-of-paimogo-composition-performance-replication/> (accessed on 4 January 2023).
8. Veiga, M.R.; Fragata, A.; Velosa, A.; Magalhães, A.C.; Margalha, G. Substitution mortars for application in historical buildings exposed to sea environment. Analysis of the viability of several types of compositions. In Proceedings of the MEDACHS’ 08—1st International Conference on Construction Heritage in Coastal and Marine Environments: Damage, Diagnostics, Maintenance and Rehabilitation, Lisboa, Portugal, 28–30 January 2008; LNEC: Lisboa, Portugal, 2008.
9. Groot, C.; Gunneweg, J. Choosing mortars compositions for repoint mortars of historic masonry under severe environmental conditions. In Proceedings of the HMC2013—3rd Historic Mortar Conference, Scotland, Glasgow, 11–14 September 2013.
10. Papayianni, I. Criteria and methodology for manufacturing compatible repair mortars and bricks. In *Compatible Materials Recommendations for the Preservation of European Cultural Heritage*; National Technical University: Athens, Greece, 1998.

11. Moropoulou, A.; Bakolas, A. Range of acceptability limits of physical, chemical and mechanical characteristics deriving from the evaluation of historic mortars. In *Compatible Materials Recommendations for the Preservation of European Cultural Heritage*; National Technical University: Athens, Greece, 1998.
12. Veiga, M.R. Air lime mortars: What else do we need to know to apply them in conservation and rehabilitation interventions? A review. *Constr. Build. Mater.* **2017**, *157*, 132–140. [[CrossRef](#)]
13. Groot, C.; Veiga, R.; Papayianni, I.; Van Hees, R.; Secco, M.; Alvarez, J.I.; Faria, P.; Stefanidou, M. RILEM TC 277-LHS report: Lime-based mortars for restoration—a review on long-term durability aspects and experience from practice. *Mater. Struct.* **2022**, *55*, 245. [[CrossRef](#)]
14. Veiga, M.D.R.; Silva, A.S. Mortars. In *Long-Term Performance and Durability of Masonry*, 1st ed.; Ghiassi, B., Lourenço, P.B., Eds.; Structures Woodhead Publishing Series in Civil and Structural Engineering; Woodhead Publishing: Sawston, UK, 2019; pp. 169–208. [[CrossRef](#)]
15. Veiga, M.R.; Velosa, A.L.; Magalhães, A.C. Evaluation of mechanical compatibility of renders to apply on old walls based on a restrained shrinkage test. *Mater. Struct.* **2006**, *40*, 1115–1126. [[CrossRef](#)]
16. Veiga, M.D.R.; Fragata, A.; Velosa, A.L.; Magalhães, A.C.; Margalha, G. Lime-Based Mortars: Viability for Use as Substitution Renders in Historical Buildings. *Int. J. Arch. Heritage* **2010**, *4*, 177–195. [[CrossRef](#)]
17. Veiga, M.R.; Aguiar, J. *Rehabilitation of S. Bruno Fort. Notes on the Results of the Collaboration Provided by LNEC to CMO*; (Reabilitação do Forte de S. Bruno. Notas sobre os resultados da colaboração prestada pelo LNEC à CMO); IV Encontro Nacional de Municípios com Centro Histórico: Oeiras, Portugal, 1996. (In Portuguese)
18. Lorient, Antoine-Joseph, 1716-1782—Mémoire sur une Découverte dans l'art de bâtir. De L'imprimerie de Michel Lambert, rue de la Harpe, près Saine Côme, Paris, 1774. (In French). Available online: <https://archive.org/details/mmoiresurunedcou00lori/mode/2up> (accessed on 9 January 2023).
19. Magalhães, A.C.; Muñoz, R.; Oliveira, M.M. O uso da mistura de cal viva e cal extinta nas argamassas antigas: O método Lorient. In *HCLB—I Congresso Internacional de História da Construção Luso-Brasileiro, Vitória, Brasil, 4–6 September 2013*; Federal University of Espírito Santo: Vitoria, Brasil, 2013. (In Portuguese)
20. Stefanidou, M.; Tsardaka, E.C.; Pavlidou, E. Influence of nano-silica and nano-alumina in lime-pozzolan and lime-metakaolin binders. *Mater. Today Proc.* **2017**, *4*, 6908–6922. [[CrossRef](#)]
21. Alvarez, J.; Fernández, J.; Navarro-Blasco, I.; Duran, A.; Sirera, R. Microstructural consequences of nanosilica addition on aerial lime binding materials: Influence of different drying conditions. *Mater. Charact.* **2013**, *80*, 36–49. [[CrossRef](#)]
22. Duran, A.; Navarro-Blasco, I.; Fernández, J.; Alvarez, J. Long-term mechanical resistance and durability of air lime mortars with large additions of nanosilica. *Constr. Build. Mater.* **2014**, *58*, 147–158. [[CrossRef](#)]
23. Ergenç, D.; Sierra-Fernandez, A.; Barbero-Barrera, M.D.M.; Gomez-Villalba, L.S.; Fort, R. Assessment on the performances of air lime-ceramic mortars with nano-Ca(OH)₂ and nano-SiO₂ additions. *Constr. Build. Mater.* **2020**, *232*, 117163. [[CrossRef](#)]
24. Stefanidou, M. The role of nanoparticles to salt decay of mortars. In *Proceedings of the 8th International Symposium on the Conservation of Monuments in the Mediterranean Basin, Rio, Greece, 31 May–2 June 2010*.
25. Papayianni, I.; Pacht, V.; Stefanidou, M. Experimental study of nano-modified lime-based grouts. *World J. Eng.* **2012**, *9*, 501–508. [[CrossRef](#)]
26. Diaz, J.; Ševčík, R.; Mácová, P.; Menéndez, B.; Frankeová, D.; Slížková, Z. Impact of nanosilica on lime restoration mortars properties. *J. Cult. Heritage* **2022**, *55*, 210–220. [[CrossRef](#)]
27. Barberena-Fernández, A.; Blanco-Varela, M.; Carmona-Quiroga, P. Use of nanosilica- or nanolime-added TEOS to consolidate cementitious materials in heritage structures: Physical and mechanical properties of mortars. *Cem. Concr. Compos.* **2019**, *95*, 271–276. [[CrossRef](#)]
28. Veiga, M.R.; Velosa, A.; Magalhães, A. Experimental applications of mortars with pozzolanic additions: Characterization and performance evaluation. *Constr. Build. Mater.* **2009**, *23*, 318–327. [[CrossRef](#)]
29. Grilo, J.; Silva, A.S.; Faria, P.; Gameiro, A.; Veiga, R.; Velosa, A. Mechanical and mineralogical properties of natural hydraulic lime-metakaolin mortars in different curing conditions. *Constr. Build. Mater.* **2014**, *51*, 287–294. [[CrossRef](#)]
30. Gameiro, A.; Silva, A.S.; Faria, P.; Grilo, J.; Branco, T.; Veiga, R.; Velosa, A. Physical and chemical assessment of lime-metakaolin mortars: Influence of binder:aggregate ratio. *Cem. Concr. Compos.* **2014**, *45*, 264–271. [[CrossRef](#)]
31. Silva, A.S.; Gameiro, A.; Grilo, J.; Veiga, R.; Velosa, A. Long-term behavior of lime-metakaolin pastes at ambient temperature and humid curing condition. *Appl. Clay Sci.* **2014**, *88–89*, 49–55. [[CrossRef](#)]
32. Veiga, M.R.; Magalhães, A.C. *Substitution External Rendering of São Jorge dos Oitavos Fortress, in Cascais: Selection of the Rendering Solution (Revestimentos Exteriores de Substituição do Forte dos Oitavos em Cascais: Seleção da Solução de Revestimento)*; Report LNEC 72/2006—DED/NRI; LNEC: Lisboa, Portugal, 2006; 17p. (In Portuguese)
33. Veiga, M.R. Conservation of historic renders and plasters: From laboratory to site. In *Historic Mortars, RILEM Book Series*; Válek, J., Hughes, J., Groot, C., Eds.; Springer: Dordrecht, The Netherlands, 2012; Volume 7, pp. 207–225. [[CrossRef](#)]
34. TC 203-RHM (Main author: Caspar Groot). RILEM TC 203-RHM: Repair mortars for historic masonry: Performance requirements for renders and plasters. *Mater. Struct.* **2012**, *45*, 1277–1285. [[CrossRef](#)]
35. Margalha, G.; Veiga, R.; Silva, A.S.; de Brito, J. Traditional methods of mortar preparation: The hot lime mix method. *Cem. Concr. Compos.* **2011**, *33*, 796–804. [[CrossRef](#)]

36. Pavía, S.; Caro, S. An investigation of Roman mortar technology through the petrographic analysis of archaeological material. *Constr. Build. Mater.* **2008**, *22*, 1807–1811. [[CrossRef](#)]
37. Bakolas, A.; Biscontin, G.; Moropoulou, A.; Zendri, E. Characterization of the lumps in the mortars of historic masonry. *Thermochim. Acta* **1995**, *269–270*, 809–816. [[CrossRef](#)]
38. EN 1015-2; Methods of Test for Mortar for Masonry. Part 2: Bulk sampling of mortars and preparation of test mortars; European Committee for Standardization CEN: Brussels, Belgium, 1998.
39. EN 1015-3; Methods of Test for Mortar for Masonry. Part 3: Determination of consistence of fresh mortar (by flow table); European Committee for Standardization CEN: Brussels, Belgium, 1999.
40. EN 1015-6; Methods of Test for Mortar for Masonry. Part 6: Determination of bulk density of fresh mortar; European Committee for Standardization CEN: Brussels, Belgium, 1998.
41. EN 1015-10; Methods of Test for Mortar for Masonry. Part 10: Determination of dry bulk density of hardened mortar; European Committee for Standardization CEN: Brussels, Belgium, 1999.
42. EN 1936; Natural Stone Test Methods. Determination of real density and apparent density, and of total and open porosity; European Committee for Standardization CEN: Brussels, Belgium, 2006.
43. EN 1015-11; Methods of Test for Mortar for Masonry. Part 11: Determination of flexural and compressive strength of hardened mortar; European Committee for Standardization CEN: Brussels, Belgium, 1999.
44. EN 14146; Natural Stone Test Methods. Determination of the dynamic modulus of elasticity (by measuring the fundamental resonance frequency); European Committee for Standardization CEN: Brussels, Belgium, 2004.
45. EN 15801; Conservation of Cultural Property. Test methods: Determination of water absorption by capillarity; European Committee for Standardization CEN: Brussels, Belgium, 2009.
46. EN 16322; Conservation of Cultural Heritage. Test methods: Determination of drying properties; European Committee for Standardization CEN: Brussels, Belgium, 2013.
47. Westerholm, M.; Lagerblad, B.; Silfwerbrand, J.; Forssberg, E. Influence of fine aggregate characteristics on the rheological properties of mortars. *Cem. Concr. Compos.* **2008**, *30*, 274–282. [[CrossRef](#)]
48. Santos, A.R.; Veiga, M.R.; Santos Silva, A.; de Brito, J. Impact of aggregates on fresh mortars' properties. In Proceedings of the 5th Historic Mortars Conference—RILEM Proceedings PRO 130, Pamplona, Spain, 19–21 June 2019; Alvarez, J.I., Fernández, J.M., Navarro, I., Durán, A., Sirera, R., Alvarez, J.I., Eds.; RILEM Publications S.A.R.L: Paris, France, 2019; pp. 1180–1194, ISBN 978-2-35158-221-3.
49. Yahia, A.; Tanimura, M.; Shimoyama, Y. Rheological properties of highly flowable mortar containing limestone filler-effect of powder content and W/C ratio. *Cem. Concr. Res.* **2005**, *35*, 532–539. [[CrossRef](#)]
50. Smith, M.R.; Collis, L. *Aggregates: Sand, Gravel and Crushed Rock Aggregates for Construction Purposes*, 3rd ed.; Geological Society of London, Engineering Geology Special Publication: London, UK, 2001. [[CrossRef](#)]
51. Snehal, K.; Das, B. Pozzolanic reactivity and drying shrinkage characteristics of optimized blended cementitious composites comprising of Nano-Silica particles. *Constr. Build. Mater.* **2022**, *316*, 125796. [[CrossRef](#)]
52. Lanás, J.; I Alvarez-Galindo, J. Masonry repair lime-based mortars: Factors affecting the mechanical behavior. *Cem. Concr. Res.* **2003**, *33*, 1867–1876. [[CrossRef](#)]
53. Santos, A.R.; Veiga, M.D.R.; Silva, A.S.; de Brito, J.; Álvarez, J.I. Evolution of the microstructure of lime based mortars and influence on the mechanical behaviour: The role of the aggregates. *Constr. Build. Mater.* **2018**, *187*, 907–922. [[CrossRef](#)]
54. Mindess, S.; Young, J.F.; Darwin, D. *Concrete*, 2nd ed.; Prentice Hall: Upper Saddle River, NJ, USA, 2002; ISBN 978-1-3064-6323.
55. Santos, A.R.; Veiga, M.D.R.; Silva, A.S.; de Brito, J. Microstructure as a critical factor of cement mortars' behaviour: The effect of aggregates' properties. *Cem. Concr. Compos.* **2020**, *111*, 103628. [[CrossRef](#)]
56. Jennings, H.M.; Bullard, J.W.; Thomas, J.J.; Andrade, J.E.; Chen, J.J.; Scherer, G.W. Characterization and Modeling of Pores and Surfaces in Cement Paste. *J. Adv. Concr. Technol.* **2008**, *6*, 5–29. [[CrossRef](#)]
57. Rosado, T.; Reis, A.; Mirão, J.; Candeias, A.; Vandenabeele, P.; Caldeira, A.T. Pink! Why not? On the unusual colour of Évora Cathedral. *Int. Biodeterior. Biodegrad.* **2014**, *94*, 121–127. [[CrossRef](#)]
58. Schabereiter-Gurtner, C.; Piñar, G.; Vybiral, D.; Lubitz, W.; Rölleke, S. Rubrobacter -related bacteria associated with rosy discolouration of masonry and lime wall paintings. *Arch. Microbiol.* **2001**, *176*, 347–354. [[CrossRef](#)]

Disclaimer/Publisher's Note: The statements, opinions and data contained in all publications are solely those of the individual author(s) and contributor(s) and not of MDPI and/or the editor(s). MDPI and/or the editor(s) disclaim responsibility for any injury to people or property resulting from any ideas, methods, instructions or products referred to in the content.